Tribology International 123 (2018) 325–328

Contents lists available at ScienceDirect

Tribology International

journal homepage: www.elsevier.com/locate/triboint

Short Communication

Variation in zinc dialkyldithiophosphate yield strength measured by nanopillar compression

Lin Feng[a,*], Rui Hao[a], Sander Gaemers[b], Christopher P. Warrens[b], Shen J. Dillon[a]

[a] University of Illinois at Urbana-Champaign, Urbana, IL, 61801, United States
[b] BP Technology Centre, Whitchurch Hill, Pangbourne, Berkshire, RG8 7QR, United Kingdom

ARTICLE INFO

Keywords:
ZDDP
In situ compression
Local chemistry effect
Mechanical properties

ABSTRACT

In situ transmission electron microscopy based nanopillar compression is utilized to investigate the mechanical properties of zinc dialkyldithiophosphate (ZDDP) tribological films. Small scale testing provides localized insights into the properties of ZDDP films that spatially vary in composition at the nanoscale. Large variations in yield strength, between 0.82 and 4.8 GPa, are measured and correlated with local chemistry changes. Lower density regions of the film that tend to be carbon-rich have lower yield stresses, than higher density regions that tend to be zinc-, iron-, and sulfur-rich. It is hypothesized that the strong compositional dependence in mechanical properties at the nanoscale is an important factor contributing to the efficacy of ZDDP as an antiwear tribological film.

1. Introduction

Eliminating zinc dialkyldithiophosphate (ZDDP) additives from lubricants has been a major goal since the introduction of stringent emissions standards, because S and P originating from ZDDP tend to poison metallic nanoparticle catalysts in catalytic converters [1]. ZDDP forms a tribological film in situ during wear at asperity contacts between surfaces. The antiwear efficacy of this tribofilm is unmatched by alternative molecules and compounds [2–4]. Unfortunately, the properties of ZDDP and its tribofilms that contribute to its exceptional antiwear behavior are not well understood. Elucidating the key physical properties of ZDDP tribofilms and their relation to tribofilm performance is an important yet incomplete step necessary for mechanism informed design of new tribofilm forming additive chemistries [3,5–10]. For example, performance metrics such as coefficient of friction and wear rate depend on underlying materials properties like hardness, yield stress, modulus, etc. The chemistry and properties of ZDDP films are spatially heterogeneous, which frustrates efforts to isolate tribofilm properties and relate them to tribofilm performance. For example, nanoindentation hardness values have been reported in the literature ranging from 1 to 10 GPa [6,11–19]. While adjacent indentations produce similar hardness values [16], significant variation is noted within single studies and between different investigators [6,11–19]. However, nanoindentation is not ideal for characterizing ZDDP tribofilms for two important reasons. First, nanoindentation hardness measurements obtained from thin films can be sensitive to the properties of the underlying substrate if the indentation depth is greater than ≈10% of the film thickness. ZDDP tribofilm thickness varies spatially between 10s of nanometers and 100s of nanometers. When performing nanoindentation the ZDDP film thickness is unknown and thus accounting for this factor is difficult. The substrate effect could skew measured results leaving some uncertainty. Second, the overall plastic volume surrounding an indent is considerably larger than the indent depth. The properties and chemistry vary spatially on a length scale that can be comparable to the plastic volume [12,20]. Therefore, indentation measurements may not capture the true variability in properties.

In a prior effort, the authors grew model ZDDP films on SiO_2 under 1 μm diamond single asperity contact using controlled loads applied by a nanomechanical tester. The mechanical properties of these films were then tested via nanopillar compression [21]. The yield stresses of the pillars reduced as the applied normal load under which the tribofilms were grown increased. Increasing the applied normal load during tribofilm growth also caused the tribofilms to become more C-rich [21]. While the growth of bulk tribofilms is complex and depends on contributions for normal stresses, shear stresses, coefficient of friction, wear regime, etc [22,23]. It was hypothesized that the variations observed in the model experiments could help explain the reported variations in nanoindentation hardness within the literature [6,11–19]. Similar results have been obtained from hardness measurements of bulk ZDDP samples grown at different loads [18]. It was hypothesized that the mixture of high strength and low strength regions resulted in a

* Corresponding author.
E-mail address: linfeng3@illinois.edu (L. Feng).

https://doi.org/10.1016/j.triboint.2018.03.020
Received 1 February 2018; Received in revised form 18 March 2018; Accepted 19 March 2018
Available online 22 March 2018
0301-679X/ Published by Elsevier Ltd.

nanocomposite that provides ZDDP tribofilms with their unique properties. The goal of this work is to confirm whether such variations in properties are observed when measuring small volumes of ZDDP tribofilms isolated from material grown under bulk metal-metal contact in a reciprocating rig, which will produce significant variations in nanoscale asperity contacts and growth stresses [22,23].

2. Materials and methods

A ZDDP tribofilm was deposited from a solution of a commercial secondary alkyl ZDDP in Group III base oil at 800 ppm phosphorus. The lubricant was placed between an SAE AMS 6440 steel substrate and a fixed ball bearing in a PCS Ltd. HFRR tester. Samples were grown under the following conditions; sequential 60, 90 and 120 °C steps for 900 s each with a maximum contact stress of 1 GPa. The test conditions were designed to model those of the most severe area of an engine, namely the contacts within the valve train. At a mean contact stress of 0.7 GPa, and with typical boundary friction values, this corresponds to a mean shear stress in the contact of ≈0.09 GPa. Wear in these tests is consistent with a normal abrasive/corrosive wear process with values of specific wear rate of approximately 1×10^{-16} m^3/Nm. The samples were rinsed with heptane prior to drying under vacuum. The process is anticipated to have limited effect on the structure and chemistry of the underlying ZDDP tribofilm. The reciprocating rig produced a wear scar ≈1500 μm long and ≈400 μm wide. Samples for subsequent analysis were prepared from the middle of the wear scar. After tribofilm growth, samples were coated with either Cu or Cr films, grown by e-beam evaporation, to protect the surface during sample preparation. This metal layer was subsequently ion milled in order to prepare a flat surface to contact during pillar compression to enable the application of a uniform stress to the underlying ZDDP film. Pillars for nanocompression and thin lamellae for scanning transmission electron microscopy (STEM) characterization were prepared by focused ion beam (FIB) lift-out techniques. Specimens were prepared from distinct regions of samples to capture spatial variation in properties. Specimens removed for nanopillar preparation were placed onto the plateau of a wedge-shaped Si substrate and bonded using ion-beam deposited platinum. Cylindrical pillars were prepared using an annular milling routine in a FIB. All specimens were prepared using Ga^+ ions at a final milling voltage of 5 keV (FEI Helios 600i). Nanopillar compression was performed using a Hysitron PI-95 picoindentor in a STEM (JEOL, 2010 F). Nanopillar compression was performed under displacement control at a constant rate of 1 nm s^{-1}. Thin specimens were characterized by energy dispersive spectroscopy (EDS) via STEM (JEOL, 2010 F).

3. Results and discussion

Fig. 1 shows a high angular annular dark-field (HAADF) STEM image of the tribofilm on the steel substrate, along with the Cu capping layer visible. The image provides atomic number contrast, where heavy elements are relatively bright and light elements are relatively dark. Considerable mixing of the steel and ZDDP are observed, likely resulting from redeposition and incorporation of wear debris. An accompanying STEM EDS map shows significant variation in the local composition of the ZDDP film. This map was taken from a region associated with redeposition of a third body layer where a large region of tribofilm could be isolated. To provide representative data of thin tribofilm regions, Fig. 2 also plots a distribution of compositions measured from a series of points acquired from various regions of the specimen. The relative amounts of Zn, Cu, Fe, S, P, and C vary considerably amongst the different points. Cu signal results from the Cu film and Cu sample mount, and varies with proximity to these components. Bright regions in the STEM image, i.e. high density, tend to be Zn-, Fe-, and S-rich, while the darker regions, i.e. low density, tend to be C-rich. This is observed in both the EDS point scans and the maps, obtained from thin layers of ZDDP deposited directly onto the substrate and thicker redeposited third body layers. EDS mapping and point acquisitions were not applied to the pillars tested by nanocompression in order to avoid associated exposure to large electron doses, which could damage the pillars and possibly effect their properties. Image contrast, which correlates with density in the amorphous pillars, provides qualitative information about local chemistry. Density varies with both chemistry and local bond distances, but we anticipate that the former is dominating the observed image contrast.

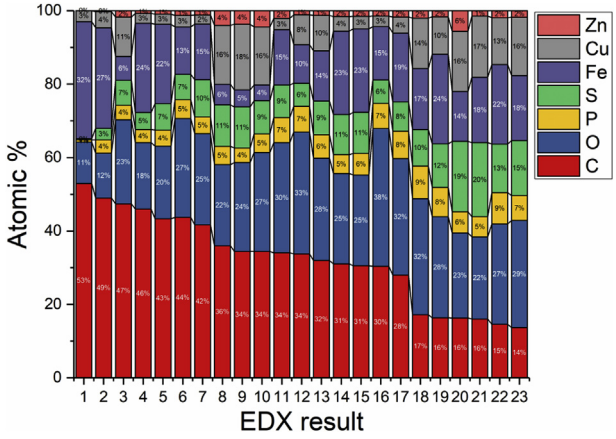

Fig. 2. Elements distribution in ZDDP rich region measured by EDX.

Fig. 3 shows two examples of in situ bright-field TEM imaging during ZDDP nanopillar deformation and associated load-displacement curves. In the first example, Fig. 3(a), the ZDDP yield stress is measured from the onset of deformation in ZDDP as indicated by the arrow in

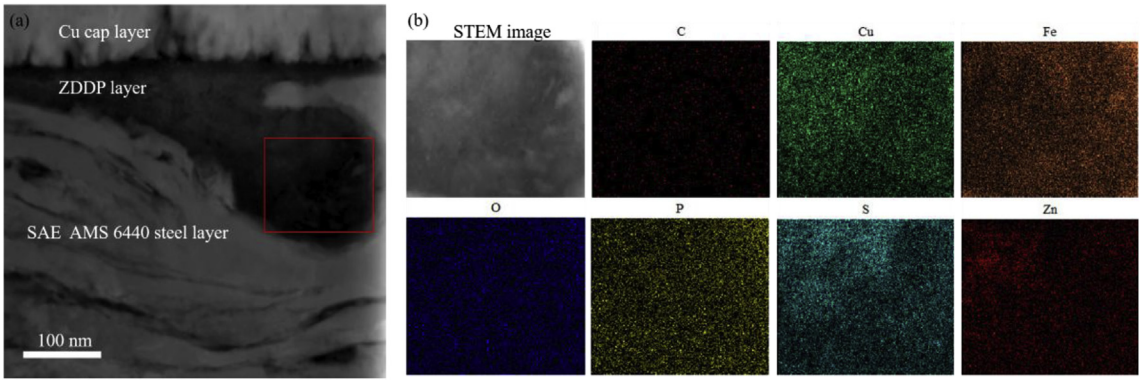

Fig. 1. High angular annular dark-field STEM image in (a) and associated EDS element maps of C, Cu, Fe, O, P, S and Zn in (b). The EDS maps in (b) were taken from the red box overlaid on the image in (a). (For interpretation of the references to colour in this figure legend, the reader is referred to the Web version of this article.)

Download English Version:

https://daneshyari.com/en/article/7001746

Download Persian Version:

https://daneshyari.com/article/7001746

Daneshyari.com